re-BUS

You have downloaded a document from
RE-BUŚ
repository of the University of Silesia in Katowice

Title: Structural and Electronic Properties of Qatranaite

Author: Anna Majtyka-Piłat, Dariusz Chrobak, Roman Nowak, Marcin Wojtyniak, Mateusz Dulski, Joachim Kusz, Józef Deniszczyk

Citation style: Majtyka-Piłat Anna, Chrobak Dariusz, Nowak Roman, Wojtyniak Marcin, Dulski Mateusz, Kusz Joachim, Deniszczyk Józef. (2019). Structural and Electronic Properties of Qatranaite. "Advances in Materials Science and Engineering" (Vol. 2019, Art. ID 4031823), doi 10.1155/2019/4031823

Uznanie autorstwa - Licencja ta pozwala na kopiowanie, zmienianie, rozprowadzanie, przedstawianie i wykonywanie utworu jedynie pod warunkiem oznaczenia autorstwa.

UNIWERSYTET ŚLĄSKI W KATOWICACH
Biblioteka Uniwersytetu Śląskiego
Ministerstwo Nauki i Szkolnictwa Wyższego

Hindawi
Advances in Materials Science and Engineering
Volume 2019, Article ID 4031823, 6 pages
https://doi.org/10.1155/2019/4031823

Research Article

Structural and Electronic Properties of Qatranaite

Anna Majtyka-Piłat,[1] **Dariusz Chrobak**,[1] **Roman Nowak**,[2] **Marcin Wojtyniak**,[3] **Mateusz Dulski**,[1] **Joachim Kusz**,[3] **and Józef Deniszczyk**[1]

[1]*Institute of Materials Science, University of Silesia in Katowice, 75 Pułku Piechoty 1A, 41-500 Chorzów, Poland*
[2]*Nordic Hysitron Laboratory, Department of Materials Science and Engineering, Aalto University, 00076 Espoo, Finland*
[3]*Institute of Physics, University of Silesia, Uniwersytecka 4, 40-007 Katowice, Poland*

Correspondence should be addressed to Roman Nowak; roman.nowak@aalto.fi

Received 10 December 2018; Revised 6 March 2019; Accepted 19 March 2019; Published 22 April 2019

Academic Editor: Joon-Hyung Lee

Copyright © 2019 Anna Majtyka-Piłat et al. This is an open access article distributed under the Creative Commons Attribution License, which permits unrestricted use, distribution, and reproduction in any medium, provided the original work is properly cited.

The present work addresses the atomic structure and electronic properties of a recently discovered mineral qatranaite ($CaZn_2(OH)_6{\cdot}2H_2O$). The present study was performed theoretically by means of density functional theory- (DFT-) based calculations within the frame of local density approximation (LDA) and general gradient approximation (GGA). To determine the energy band gap width, we carried out the ultraviolet-visible spectroscopy (UV-Vis) measurements. The structure relaxation performed with use of LDA and GGA provides results matching the experimentally determined crystal parameters. Interestingly, in contrast to existing interpretation of experimental data, our DFT calculations revealed energy gap of direct characteristics. Accordingly, our UV-Vis experiments yield the band gap width of 3.9 eV.

1. Introduction

Qatranaite named after the village Al Qatrana (situated 15 km southeast from the Amman Aquaba Asia-Jordan Desert Highway) is considered as a natural analogue of synthetic calcium hexahydroxodizincate dehydrate [1, 2]. The mineral, discovered in an altered pyrometamorphic spurrite rocks in the Daba-Siwaqa region of the Hatrurim complex located in Jordan [3–6], was for the first time described in 2016 by Stasiak et al. as $CaZn_2(OH)_6{\cdot}OH_2O$ [7]. Qatranaite crystallized in the temperature range 150 to 200°C, similarly as Se-bearing thaumasite or afwillite, in the form of flatten (010) crystals, growing up to 0.3 mm [7, 8].

Qatranaite unit cell consists of octahedrally coordinated Ca^{2+} ions linked to four hydroxy groups and two water molecules, whereas Zn^{2+} ions are tetrahedrally coordinated with four OH^- groups and form pyroxene-like chains $[Zn_2(OH)_6]^{2-}$. The mineral may display charge deficiency in case all oxygen atoms participate in the formation of OH groups, which certainly affects electronic properties of this interesting material [8].

The potential application of calcium hexahydroxodizincate dehydrate-like systems sparked hope for improved charge/discharge reversibility in Zn battery electrodes. Furthermore, they are expected to restrict Zn-electrode shape change and inhibit dendrite formation [1, 2, 9–11]. Additionally, electrochemical properties of $CaZn_2(OH)_6{\cdot}2H_2O$ make it suitable for negative electrodes in rechargeable zinc-air batteries [12, 13].

The energy gap of calcium hexahydroxodizincate dehydrate has been a subject of experimental investigations [2] from which the direct energy gap width of 3.1 eV has been concluded. Our UV-Vis measurements of qatranaite revealed that the spectrum can be equally well interpreted, assuming the presence of direct or indirect energy gap. In order to disclose the nature of the energy gap in the mineral, we carried out the quantum, DFT-based, electronic structure investigations by means of the pseudopotential method employed in the Quantum Espresso package [14]. To verify reliability of the calculations, we have also performed the structural optimization and compared the results with experimental data. An ab initio prediction for the energy band gap was compared with experimental results provided by UV-Vis measurements.

2. Computational and Experimental Details

An ab initio calculations were carried out using the Quantum Espresso code [14] by applying the scalar relativistic ultrasoft pseudopotentials [15] for Ca($3s^2 3p^6 4s^2$), H($1s^2$), and O($2s^2 2p^6$) elements within both LDA and GGA calculations. For Zn, we used the same type pseudopotentials with ($3d^{9.7} 4s^2 4p^{0.3}$) and ($3d^{10} 4s^2$) valence state configuration for LDA and GGA, respectively. Calculations were performed for two approximations of exchange correlation (XC) energy functional. The LDA XC functional in the form parameterized by Perdew and Zunger [16] and the GGA XC functional proposed by Perdew et al. [17] were employed. The plane wave kinetic energy and charge density cutoff of 46 and 368 Ry, respectively, were applied within LDA, while in the case of GGA, the corresponding cutoff values equaled 53 and 368 Ry. The structure-optimization, following the Broyden–Fletcher–Goldfarb-Shanno (BFGS) scheme, was carried out within LDA and GGA approaches. The usage of the $12 \times 12 \times 12$ Monkhorst–Pack mesh [18] in reciprocal space enabled us to achieve satisfactory convergence in the structural optimization. The total energy of the qatranaite unit cell was evaluated with an accuracy of 5 meV, while forces were calculated with uncertainty less than 0.08 and 5.21 meV/Å for LDA and GGA, respectively. To determine precisely the details of electronic density of states, the additional calculations using the $20 \times 20 \times 20$ Monkhorst–Pack mesh were performed.

To study the energy gap of qatranaite, the ultraviolet-visible spectroscopy (UV-Vis) was performed with the use of microspectrophotometer (CRAIC Technologies) equipped with standard halogen lamp and Zeiss 15x objective. The sample was prepared in the form of petrographic polished plate with the qatranaite crystals (diameter of 0.3 mm) embedded in the mineral matrix. The experiments were performed at room temperature and ambient pressure. To estimate the band gap width, we use the formula proposed by Wood and Tauc [19]:

$$h\nu \cdot \alpha \sim \left(h\nu - E_g\right)^n, \tag{1}$$

where α is the absorbance, h stands for the Planck constant, ν defines the photon's frequency, E_g denotes the optical band gap energy, and n is a constant related to different kinds of electronic transitions. The n parameter equals 0.5, 2, 1.5, and 3 for direct, indirect, allowed, and forbidden transitions, respectively.

3. Results and Discussion

3.1. Structural Properties. According to the experimental results provided by Stasiak et al. [7], the $CaZn_2(OH)_6{\cdot}2H_2O$ mineral crystallizes in the $P2_1/c$-type structure with the following lattice parameters: $a = 6.3889(8)$ Å, $b = 10.969(1)$ Å, $c = 5.7588(8)$ Å, and $\beta = 101.95(1)^\circ$. The coordination of each Zn atom to four oxygen atoms and Ca atom to six oxygen atoms prompted the authors to imagine the qatranaite unit cell as a particular set of tetrahedral ZnO_4 and octahedral CaO_6 clusters (Figure 1). Peculiarity of the qatranaite unit cell is related to the presence of hydroxyl groups [OH] attached to hydrogen bridges to H_2O molecules [20], which ensures the electric charge balance.

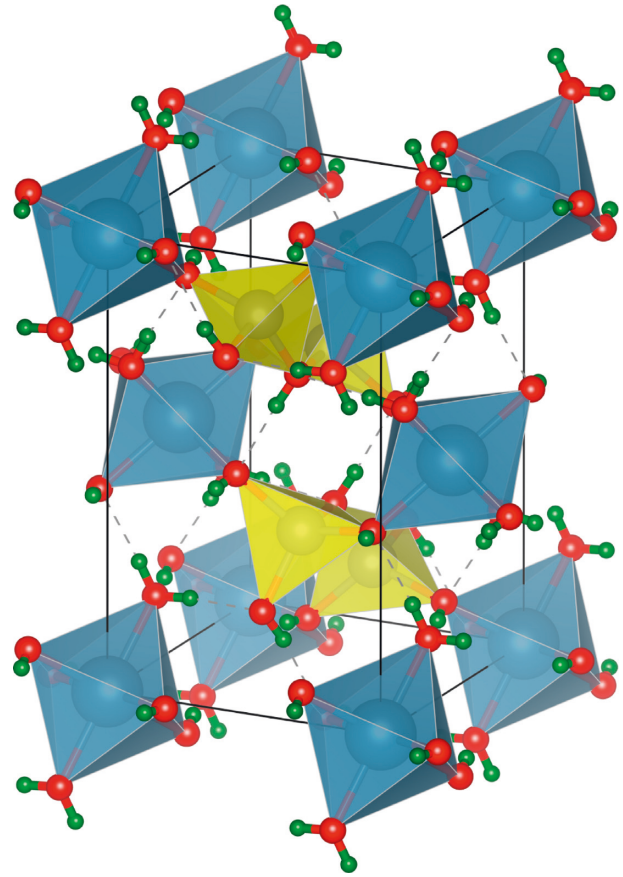

Figure 1: Schematic of the crystalline structure of qatranaite showing the tetrahedrally coordinated zinc (ZnO_4; yellow) and octahedrally coordinated calcium (CaO_6; blue) clusters. The red and green spheres denote oxygen and hydrogen atoms, respectively.

Tables 1 and 2 summarize the results of ab initio structural optimization of qatranaite unit cell carried out with the use of two approximations for XC energy functional. The calculated results were compared with available experimental data. It is worth emphasizing that the output of DFT-LDA calculations is in well agreement with the previously reported diffraction data [7, 8] (Table 1). The computed (LDA) and measured a, b, c lattice parameters and β angle differ less than 0.2, 2.3, 3.5, and 2.1%, respectively. GGA approach give slightly worse results (corresponding differences are 4.1, 2.9, 5.6, and 0.6%). It can be concluded that LDA XC functional better describes the nature of bonding in qatranaite.

In Table 2, we compare experimental and optimized coordinates of Wyckoff positions in the structure of $CaZn_2(OH)_6{\cdot}2H_2O$ mineral. To avoid the issue of high mobility of hydrogen atoms [21], their experimentally obtained coordinates were frozen during structural optimization. We are satisfied with the overall agreement between calculated and measured coordinates of Wyckoff positions [8]. The noticeable difference in Wyckoff position can be observed for oxygen atoms, which may be attributed to their relative high mobility [22].

Table 1: Lattice parameters of qatranaite estimated with the LDA and GGA and compared with the measured values.

Parameters	LDA	GGA	Exp. [7]
a (Å)	6.388	6.652	6.389
b (Å)	10.720	11.286	10.969
c (Å)	5.960	6.081	5.759
β (°)	104.05	102.52	101.95

Table 2: Experimental and calculated coordinates of Wyckoff positions in qatranaite single crystal.

Atom	Exp. [8]			DFT-LDA			DFT-GGA		
	X	Y	Z	x	Y	z	x	y	z
Zn1-4*e*	0.5332	0.6650	0.6639	0.5300	0.6670	0.6385	0.5313	0.6669	0.6536
O1-4*e*	0.4687	0.6814	0.3122	0.4451	0.6933	0.3030	0.4540	0.6891	0.3108
H1-4*e*	0.5227	0.61710	0.2675	—	—	—	—	—	—
O2-4*e*	0.3380	0.5427	0.7455	0.3557	0.5309	0.7117	0.3440	0.5363	0.7084
H2-4*e*	0.3226	0.5543	0.8576	—	—	—	—	—	—
O3-4*e*	0.8349	0.6236	0.7394	0.8377	0.6388	0.6993	0.8311	0.6308	0.7010
H3-4*e*	0.8739	0.6108	0.85960	—	—	—	—	—	—
O4-4*e*	0.0373	0.6603	0.2367	0.0206	0.6422	0.2193	0.0262	0.6486	0.2274
H4-4*e*	0.1712	0.6704	0.2490	—	—	—	—	—	—
H5-4*e*	−0.01980	0.7304	0.2400	—	—	—	—	—	—
Ca1-2a	0.0000	0.0000	0.0000	0.0000	0.0000	0.0000	0.0000	0.0000	0.0000

For hydrogen atoms, "—" stands for experimental values of coordinates.

Based on structural data collected in Table 2, we also calculated an interatomic distances in tetrahedral ZnO_4 and octahedral CaO_6 clusters. The obtained results are presented in Table 3. The comparison of DFT structural results with experimental data confirms sufficient reliability of our calculations.

3.2. Electronic Properties. Physical properties of a novel material are essential for its intended applications in electronics and photonics. Consequently, the energy band structure and the details of qatranaite's partial density of states (PDOS) are of common interest. Indeed, our DFT-determined band diagram (Figure 2) indicates the insulating property of qatranaite with a direct band gap, at the Γ-point of reciprocal k-lattice, of 3.2 eV (LDA) and 3.3 eV (GGA).

Closer inspection of Figure 2 reveals that the selection of LDA and GGA of exchange-correlation energy does not significantly affect the shape of energy bands. Furthermore, the partial DOS analysis (Figure 3) reveals the electronic states near the top of the valence-band filled by O-p and Zn-d electrons with slight contribution of Ca electrons.

3.3. UV-Vis Absorption Spectroscopy. The results obtained from our DFT calculations demonstrated that qatranaite is the direct band gap material, and consequently, the n value of 0.5 have to be used in equation (1). The energy band gap, $E_g = 3.9$ eV, was estimated by fitting equation (1) to the experimental points at the linear portion of the curve (Figure 4). The latter value exceeds the one deduced from DFT calculations ($E_g = 3.2$ eV). This confirms the common perception that DFT calculations frequently lead to

Table 3: Interatomic distances in ZnO_4 and CaO_6 clusters.

	Interatomic distances (Å)									
	Zn1						Ca1			
	O1	O1	O2	O3	O2	O2	O3	O3	O4	O4
LDA	1.96	1.94	1.95	1.93	2.34	2.34	2.29	2.30	2.30	2.29
GGA	2.05	2.00	2.00	1.99	2.40	2.40	2.39	2.35	2.35	2.39
Exp. [7]	1.91	1.99	1.95	1.94	2.37	2.37	2.37	2.34	2.34	2.34

The atomic symbols (e.g., O1 and O2) denote atoms occupying different Wyckoff positions.

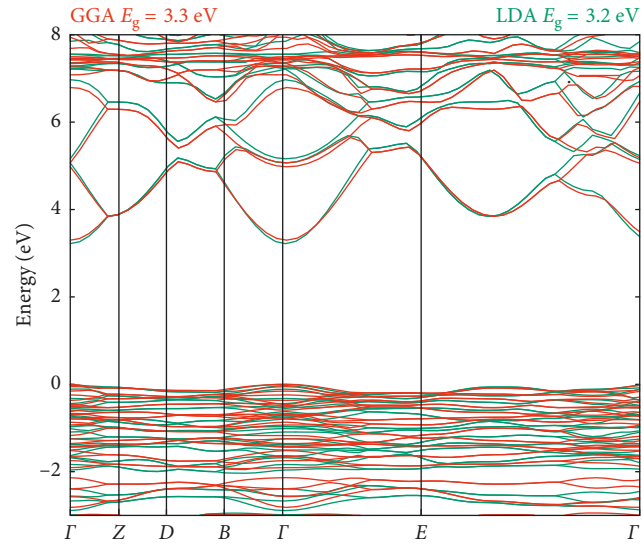

Figure 2: The electronic band structure of crystalline qatranaite determined within LDA (green lines) and GGA (red lines). The zero of the energy scale is shifted to the top of the valence band.

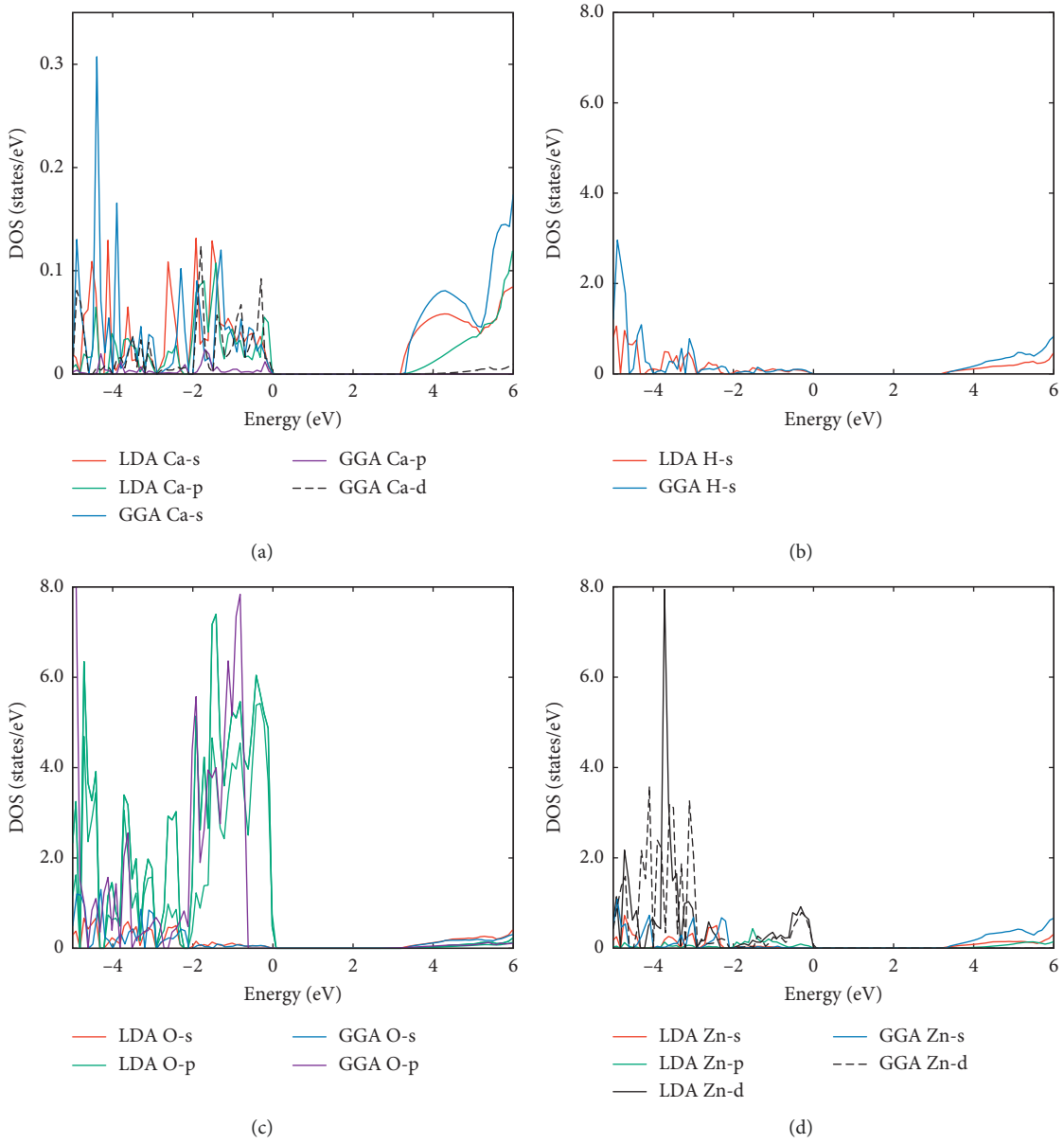

Figure 3: Partial density of states determined for qatranaite. The zero of the energy scale is shifted to the top of the valence band.

underestimation of the band gap [23]. Therefore, it may be concluded that the true energy gap in qatranaite should significantly exceed the calculated DFT value.

Finally, the calculations and experimental results obtained for natural qatranaite were compared with previously published data for synthetic counterpart [2]. Thus, Xavier et al. measured the energy gap E_g of 3.1 eV, the value significantly lower than the one obtained by our UV-Vis absorption spectroscopy measurements. Such a high discrepancy is due to disputable assumptions imposed by Xavier et al. [2], who fitted their absorption results in such a way that stipulates $n = 2$ (equation (1)). The differences between experimentally derived energy gap for qatranaite (3.9 eV) and synthetic $CaZn_2(OH)_6{\cdot}2H_2O$ (3.1 eV) [2] may stem from chemical and structure imperfections present in mineral qatranaite.

4. Conclusions

In sum, we have demonstrated the DFT calculations within LDA and GGA schemes accurately predict the atomic structure, which encourage the further study of qatranaite electronic properties. The calculated lattice parameters at the ground state conditions are in agreement with the experimental results. It is contend, therefore, that LDA is more appropriate for estimation of lattice parameters of qatranaite. The LDA (GGA) predicted direct band gap energy at Γ point of the first Brillouin zone provided the lower value 3.2 eV (3.3 eV) compared to our experimentally obtained 3.9 eV data. Moreover, it is worth noting that our theoretical and experimental results reveal the presence of direct gap in qatranaite mineral where available experimental data for its synthetic analogue pointed on indirect energy gap. We

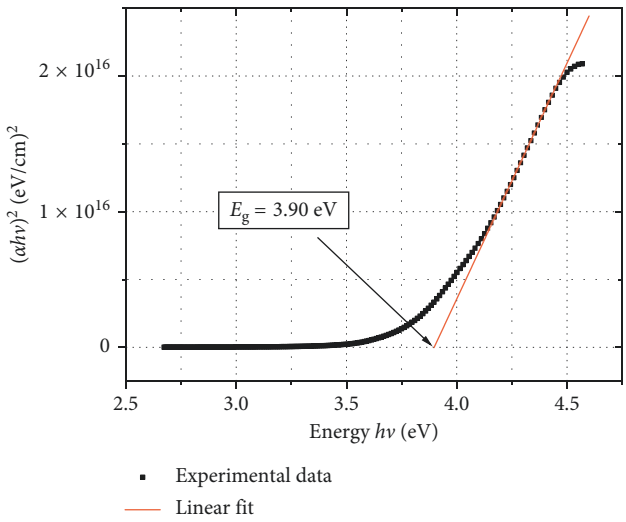

Figure 4: UV-Vis spectrum of qatranaite (black dots). Linear fit, according to equation (1), shows the energy gap width E_g.

believe that the output of our calculations contains information being of importance to the modern electronic and photonic industries.

Data Availability

The raw data from all implemented techniques (UV-VIS, DFT) used to support the findings of this study are available from the corresponding author upon request.

Disclosure

The authors would like to inform that a small part of their simulation results were previously published in a poster form.

Conflicts of Interest

The authors declare no conflicts of interest regarding the publication of this paper.

Acknowledgments

This research was partially supported by PL-Grid Infrastructure. DCH acknowledges the support from the National Science Centre of Poland (Grant no. 2016/21/B/ST8/02737).

References

[1] C.-C. Yang, W.-C. Chien, P.-W. Chen, and C.-Y. Wu, "Synthesis and characterization of nano-sized calcium zincate powder and its application to Ni-Zn batteries," *Journal of Applied Electrochemistry*, vol. 39, no. 1, pp. 39–44, 2009.

[2] C. S. Xavier, J. C. Sczancoski, L. S. Cavalcante et al., "A new processing method of $CaZn_2(OH)_6{\cdot}2H_2O$ powders: photoluminescence and growth mechanism," *Solid State Sciences*, vol. 11, no. 12, pp. 2173–2179, 2009.

[3] Y. Bentor, "Israel," in *Lexique Stratigraphique International: Asie*, vol. 3, p. 80, Centre National de la Recherche Scientifique, Paris, France, 1960.

[4] S. Gross, "The mineralogy of the Hatairim formation, Israel," *Geological Survey of Israel, Bulletin*, vol. 70, pp. 1–80, 1977.

[5] E. Sokol, I. Novikov, S. Zateeva, Y. Vapnik, R. Shagam, and O. Kozmenko, "Combustion metamorphism in the Nabi Musa dome: new implications for a mud volcanic origin of the Mottled Zone, Dead Sea area," *Basin Research*, vol. 22, no. 4, pp. 414–438, 2010.

[6] Y. Vapnik, V. Sharygin, E. Sokol, and R. Shagam, "Paralavas in a combustion metamorphic complex: Hatrurim Basin, Israel," *Geological Society of America Reviews in Engineering Geology*, vol. 18, pp. 1–21, 2007.

[7] M. Stasiak, E. V. Galuskin, J. Kusz et al., "IMA commission on new minerals nomenclature and classification (CNMNC), Qatranaite, IMA 2016-024," *Mineralogical Magazine*, vol. 80, no. 32, pp. 915–922, 2016.

[8] Y. Vapnik, E. V. Galuskin, I. O. Galuskina et al., "Qatranaite$CaZn_2(OH)_6{\cdot}2H_2O$—a new mineral from altered pyrometamorphic rocks of the Hatrurim Complex, Daba-Siwaqa, Jordan, in review," *European Journal of Mineralogy*, 2019.

[9] R. Stahl, H. Jacobs, and Z. Anorg, "Zur kristallstruktur von $CaZn_2(OH)_6{\cdot}2H_2O$," *Zeitschrift für anorganische und allgemeine Chemie*, vol. 623, no. 8, pp. 1287–1289, 1997.

[10] X. M. Zhu, H. X. Yang, X. P. Ai, J. X. Yu, and Y. L. Cao, "Structural and electrochemical characterization of mechanochemically synthesized calcium zincate as rechargeable anodic materials," *Journal of Applied Electrochemistry*, vol. 33, no. 7, pp. 607–612, 2003.

[11] J. Yu, H. Yang, X. Ai, and X. Zhu, "A study of calcium zincate as negative electrode materials for secondary batteries," *Journal of Power Sources*, vol. 103, no. 1, pp. 93–97, 2001.

[12] Y.-J. Min, S.-J. Oh, M.-S. Kim, J.-H. Choi, and S. Eom, "Calcium zincate as an efficient reversible negative electrode material for rechargeable zinc–air batteries," *Ionics*, vol. 24, pp. 1–7, 2018.

[13] A. R. Mainar, E. Iruin, L. C. Colmenares et al., "An overview of progress in electrolytes for secondary zinc-air batteries and other storage systems based on zinc," *Journal of Energy Storage*, vol. 15, no. 1, pp. 304–328, 2018.

[14] P. Giannozzi, S. Baroni, N. Bonini et al., "QUANTUM ESPRESSO: a modular and open-source software project for quantum simulations of materials," *Journal of Physics: Condensed Matter*, vol. 21, no. 39, article 395502, 2009.

[15] http://www.quantum-espresso.org/pseudopotentials/pslibrary/.

[16] J. P. Perdew and A. Zunger, "Self-interaction correction to density-functional approximations for many-electron systems," *Physical Review B*, vol. 23, no. 10, pp. 5048–5079, 1981.

[17] J. P. Perdew, K. Burke, and M. Ernzerhof, "Generalized gradient approximation made simple," *Physical Review Letters*, vol. 77, no. 18, pp. 3865–3868, 1996.

[18] H. J. Monkhorst and J. D. Pack, "Special points for Brillouin-zone integrations," *Physical Review B*, vol. 13, no. 12, pp. 5188–5192, 1976.

[19] D. L. Wood and J. Tauc, "Weak absorption tails in amorphous semiconductors," *Physical Review B*, vol. 5, no. 8, pp. 3144–3151, 1972.

[20] T.-C. Lin, M. Y. A. Mollah, R. K. Vempati, and D. L. Cocke, "Synthesis and characterization of calcium hydroxyzincate using X-ray diffraction, FT-IR spectroscopy, and scanning

force microscopy," *Chemistry of Materials*, vol. 7, no. 10, pp. 1974–1978, 1995.

[21] D. Gaspar, L. Pereira, K. Gehrke, B. Galler, E. Fortunato, and R. Martins, "High mobility hydrogenated zinc oxide thin films," *Solar Energy Materials and Solar Cells*, vol. 163, pp. 255–262, 2017.

[22] M. Boccard, N. Rodkey, and Z. C. Holman, "High-mobility hydrogenated indium oxide without introducing water during sputtering," *Energy Procedia*, vol. 92, pp. 297–303, 2016.

[23] J. P. Perdew, R. G. Parr, M. Levy, and J. L. Balduz, "Density-functional theory for fractional particle number: derivative discontinuities of the energy," *Physical Review Letters*, vol. 49, no. 23, pp. 1691–1694, 1982.